Inverse electron demand Diels-Alder pyridazine elimination: synthetic tools for chemical immunology

Geus, M.A.R. de

7

Summary and future prospects

The inverse electron demand Diels-Alder (IEDDA) pyridazine elimination[1] emerged in 2013 as a new bioorthogonal reaction and constitutes a prime example of what is now known as dissociative bioorthogonal chemistry.[2–4] The research described in this Thesis aims to develop synthetic strategies which enable the IEDDA pyridazine elimination to be applied as a versatile toolbox in chemical biology studies. More specifically, it entails modification of antigenic (MHC-I) peptides and (CD1d) glycolipids with a *trans*-cyclooctene (TCO) moiety to allow chemical control over the recognition of these biomolecules by immune cells. Synthetic advances which encompass the entire scope of the IEDDA pyridazine elimination are additionally described.

Chapter 1 introduces the IEDDA pyridazine elimination within the context of dissociative bioorthogonal chemistry. Mechanistic aspects of the reaction are discussed, as well as various applications where this technique has been utilized. An overview of other novel bioorthogonal bond cleavage reactions is presented.

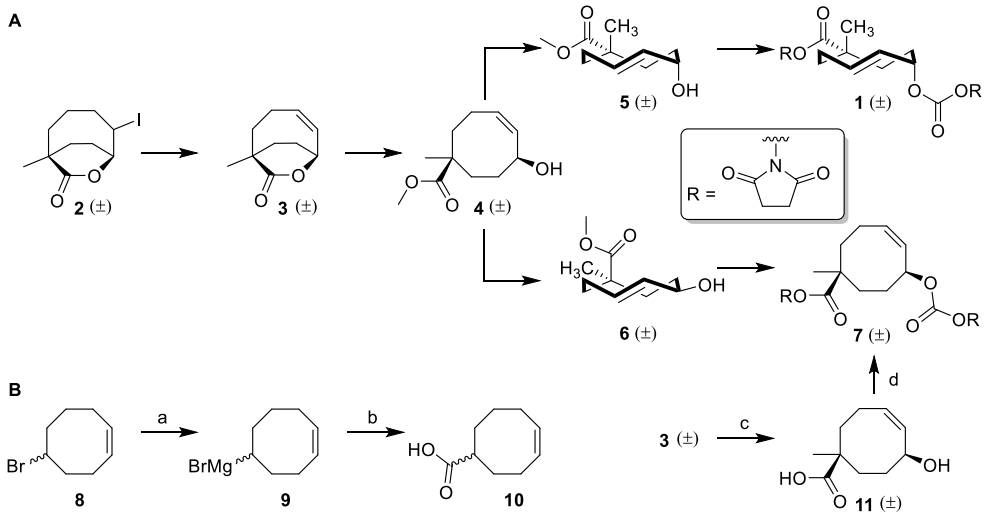

Scheme 1 A) Key intermediates in the synthesis of TCO reagent **1** and CCO reagent **7** from 1,5-cyclooctadiene as presented in Chapter 2. B) Reagents/conditions (Thurecht and co-workers)[7]: (a) Mg, THF, I_2, reflux; (b) CO_2, 65% over 2 steps; (c) KOH, MeOH; (d) N,N'-disuccinimidyl carbonate, DIPEA, MeCN, rt, 28% over 2 steps.

Chapter 2 describes a streamlined synthesis of bifunctional TCO reagent (**1**) which has been extensively applied for click to release chemistry (Scheme 1).[5,6] A key modification of existing literature procedures features the crystallization of iodolactone **2** after initial functionalization of 1,5-cyclooctadiene. Transesterification of bicyclic lactone **3** was replaced by a one pot, two step saponification-methylation procedure to obtain methyl ester **4**. Photoisomerization afforded a mixture of **5** and **6**, which could be separated after selective saponification of **5**. Bis-NHS functionalization to obtain **1** was accelerated using nucleophilic catalysis. The unprecedented *cis*-cyclooctene (CCO) reagent (**7**) was obtained by functionalization and *trans*-to-*cis* isomerization of **6**. Additionally, reagent **1** was equipped with an EDANS fluorophore and a DABCYL quencher to obtain a fluorogenic TCO-reporter-quencher probe for kinetic analysis of the IEDDA pyridazine elimination.[6]

Another route to obtain **1** was published by Thurecht and co-workers.[7] Instead of employing cyanide substitution, they converted cyclooctene bromide **8** into the corresponding Grignard reagent (**9**), which was treated with CO_2 to obtain cyclooctene carboxylic acid **10** in 65% yield over two steps. This alternative route to intermediate **10** is projected to improve the synthetic accessibility of iodolactone **2**. Additionally, the two step synthesis of CCO reagent **7** is reported from bicyclic lactone **3** in 28% yield.[7] While this finding confirms the intramolecular cyclization observed for the attempted functionalization of carboxylic acid **11**, it also shows that small quantities of CCO reagent **7** can be obtained directly.

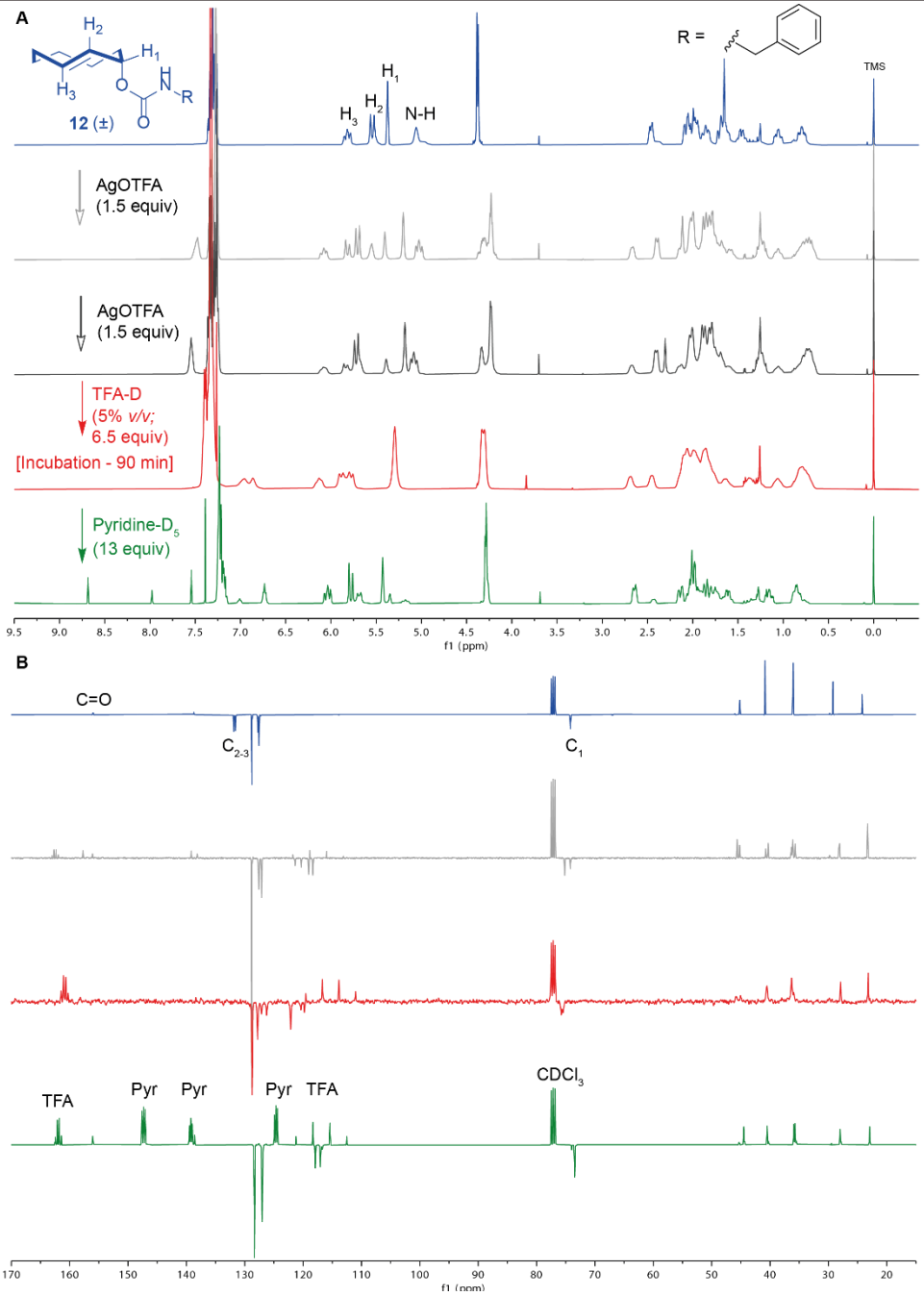

Figure 1 Stacked ^{1}H (A; δ 9.5/-0.5 ppm) and ^{13}C-APT (B; 170/15 ppm) NMR spectra of model TCO carbamate **12** before and upon treatment with AgOTFA (1.5 equiv; then another 1.5 equiv), followed by exposure to TFA-D (5% *v/v* in $CDCl_3$; 6.5 equiv). After 90 minutes, the mixture was quenched by adding pyridine-D_5 (13 equiv). Experiments in Chapter 3 (without AgOTFA addition) exposed **12** to 5/10/20% *v/v* TFA-D, resulting in an estimated stability of 94/75/<10%.

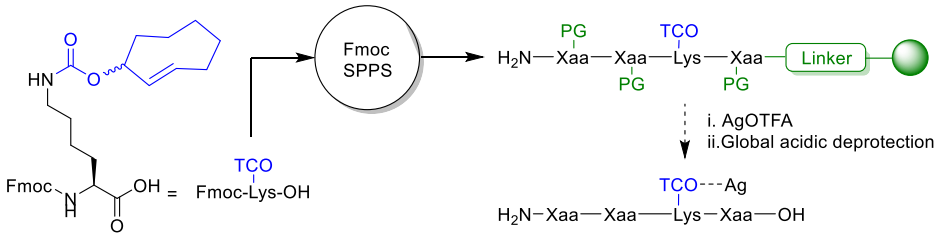

Figure 2 Proposed updated synthetic strategy for an Fmoc SPPS-based strategy for TCO-modified peptide synthesis. PG = protecting group; Xaa = unspecified amino acid.

Chapter 3 describes the attempted development of an Fmoc SPPS-based strategy for TCO-modified peptide synthesis. A model axial allylic substituted TCO carbamate (Figure 1, **12**) was studied in the presence of TFA-D using ^{1}H and ^{13}C NMR. The observed stability under dilute TFA concentrations (< 10% *v/v*) was attributed to preferential protonation on C_3 and anchimeric assistance of the carbamate moiety towards C_2 of the cationic species. An Fmoc-Lys(TCO)-OH building block was synthesized and incorporated in the SIINFEKL peptide sequence on solid support. Global deprotection of this peptide led to substantial TCO isomerization and carbamate hydrolysis, even under dilute TFA concentrations (for instance 5% *v/v*) which appeared to be tolerated in the NMR stability experiments.

Another approach to minimize isomerization of the *trans*-double bond would be to apply conditions which stabilize this moiety in the presence of acids such as TFA. It has been established that complexation of $AgNO_3$ with TCO readily occurs over binding with CCO.[8,9] This energetically favored metal complexation has previously been exploited for extractive separations,[10] but also for the isolation of TCO during photochemical synthesis[11] and to prolong the shelf-life of conformationally unstable TCOs after synthesis.[12,13] It was hypothesized that the formation of a silver-TCO complex could act as a temporary protecting group during global acidic deprotection of the peptide sequence from the solid support. Model allylic TCO **12** was treated with AgOTFA (3.0 equivalents) to obtain a diastereomeric mixture of axial TCO carbamate-Ag complexes on ^{1}H and ^{13}C NMR (Figure 1 A/B). Subsequent addition of TFA-D (5% *v/v* in $CDCl_3$; 6.5 equivalents) led to the appearance of a species which was distinct from the cationic species observed for the experiments described in Chapter 3. Furthermore, after the mixture was quenched by adding pyridine-D_5 (13 equivalents), the resulting allylic TCO appeared to be present as the TCO-Ag complex. The results of this initial NMR experiment may provide a basis for further investigations to improve the strategy proposed in Chapter 3 with the addition of AgOTFA during global acidic deprotection of peptides (Figure 2).

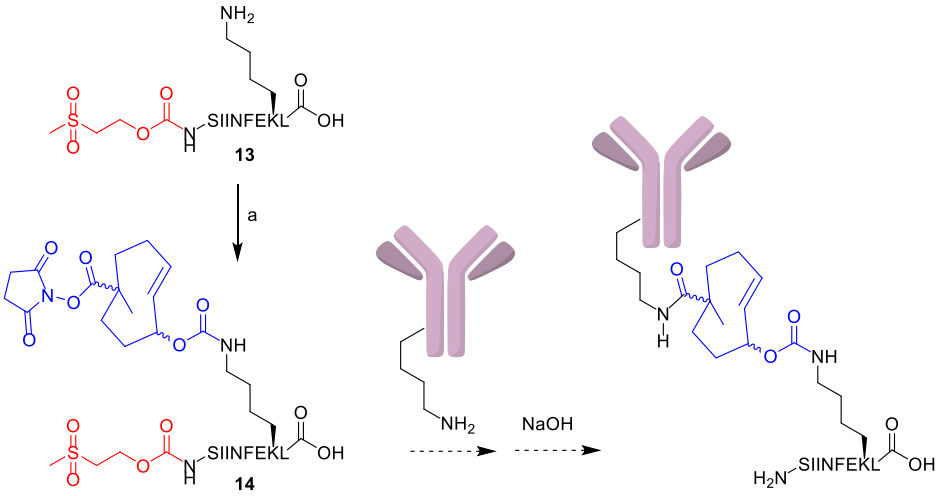

Figure 3 Proposed strategy for conjugation of caged epitopes with antibodies for improved tissue specificity of T-cell activation. Reagents/conditions: (a) NHS-bTCO (Chapter 2; **1**), DIPEA, DMF, rt, 12%.

Chapter 4 reports a new method for chemical control over T-cell activation *in vitro* and *in vivo*. MHC-I epitopes were designed with allylic substituted TCO modification on lysine residues on the premise that this modification would obstruct recognition of such epitopes by T-cells, whilst the IEDDA pyridazine elimination could selectively restore this recognition event. In contrast to the attempted synthetic method described in Chapter 3, the MHC-I peptide sequence was synthesized using Fmoc SPPS before installing the TCO moiety. N-terminal protection with the base-labile MSc-group before acidic cleavage of the peptide sequence enabled regioselective TCO modification of the ε-amino group of lysine. MSc deprotection under basic conditions was followed by HPLC purification to obtain the desired caged epitopes. Lysine-caged epitopes of $OVA_{257-264}$ (OT-I, SIINFEKL) and $D^bM_{187-195}$ (NAITNAKII) displayed binding to MHC-I whilst T-cell recognition was absent. IEDDA pyridazine elimination effectively restored T-cell activation *in vitro* and *in vivo*. In addition, the 'click to release' approach was applied to study antigen cross presentation with an N-terminally extended epitope, $OVA_{247-264}$ (DEVSGLEQLESIINFEKL).

Future developments are aimed to improve the spatiotemporal control by which the antigen recognition is switched on. This is especially important for *in vivo* experiments where high tissue specificity is desired. One way to achieve this is to attach a targeting moiety to the caged MHC-I antigen. In this regard, the bifunctional TCO scaffold initially employed to add an additional polar functionality can be repurposed to enable, for instance, the conjugation of an antibody to the caged antigen (Figure 3). To this end, MSc-SIINFEKL (Chapter 4; **13**) was reacted with bifunctional NHS-TCO (Chapter 2; **1**),

followed by HPLC purification of the resulting NHS-ester (**14**) as a reagent for lysine conjugation. Conversely, the conjugation of an antibody to a tetrazine represents an alternative strategy for tissue specific decaging, as previously shown by Du *et al*.[14]

In vitro deprotection experiments in Chapter 4 revealed 3,6-dipyrimidinyl-tetrazine does not induce detectable elimination upon IEDDA ligation. An *in vitro* 'blocking and decaging' approach, where IEDDA ligation events with a non-elimination tetrazine are followed by a kinetic window before uncaging with a regular tetrazine, would be especially valuable to delineate antigen cross presentation. In order for such a strategy to succeed, however, the 'blocking' tetrazine employed must perform IEDDA ligation on the cell surface without also affecting caged antigens which are still being processed inside the antigen presenting cell (APC). It was reasoned that (sufficiently large) polymer-modified tetrazines[15] could prevent passive cellular diffusion and would therefore enable the envisioned kinetic antigen cross presentation experiments. The addition of an exocyclic *para*-amino group on 2-pyridine and/or 2-pyrimidine substituents of electron poor tetrazines was assessed as a suitable conjugation handle for this purpose.

Cyclization of 5-amino-2-pyridine carbonitrile (**15**) and 2-pyridine carbonitrile in the presence of hydrazine hydrate afforded a crude dihydrotetrazine mixture. Subsequent oxidation in the presence of (diacetoxyiodo)benzene (BAIB)[16] afforded a mixture of **16**[17] and **17** which were separated using silica gel chromatography (Scheme 2). Acylation of **16** in the presence of glutaric anhydride required extended reaction times and a large excess of reagent to obtain **18**. Boc-protected nitrile **19** was reacted with 2-pyrimidine carbonitrile in the presence of hydrazine hydrate to obtain dihydrotetrazine **20**, which was readily isolated using silica gel chromatography. Subsequent oxidation with BAIB afforded tetrazine **21**. Deprotection of the Boc group in a mixture of HCl and dioxane afforded a complex mixture of products.

It is projected that installation of the amide bond before initiating formation of the (dihydro)tetrazine, as described by Maggi *et al.,*[18] would enhance isolation of the desired product and circumvent the poor nucleophilicity of the *para*-amino group. Conjugation of **15** and glutaric anhydride afforded **22**[18] in 80% yield. Cyclization of **22** with 2-pyridimidine carbonitrile and subsequent oxidation with BAIB would result in tetrazine **23**. In a similar manner, conjugation of 5-amino-2-cyanopyrimidine (**24**) with glutaric anhydride would afford **25**, which could be used to obtain tetrazine **26**. Tetrazines **18, 23** and **26** would be amenable for conjugation with amino functionalized dextran polymers.[5]

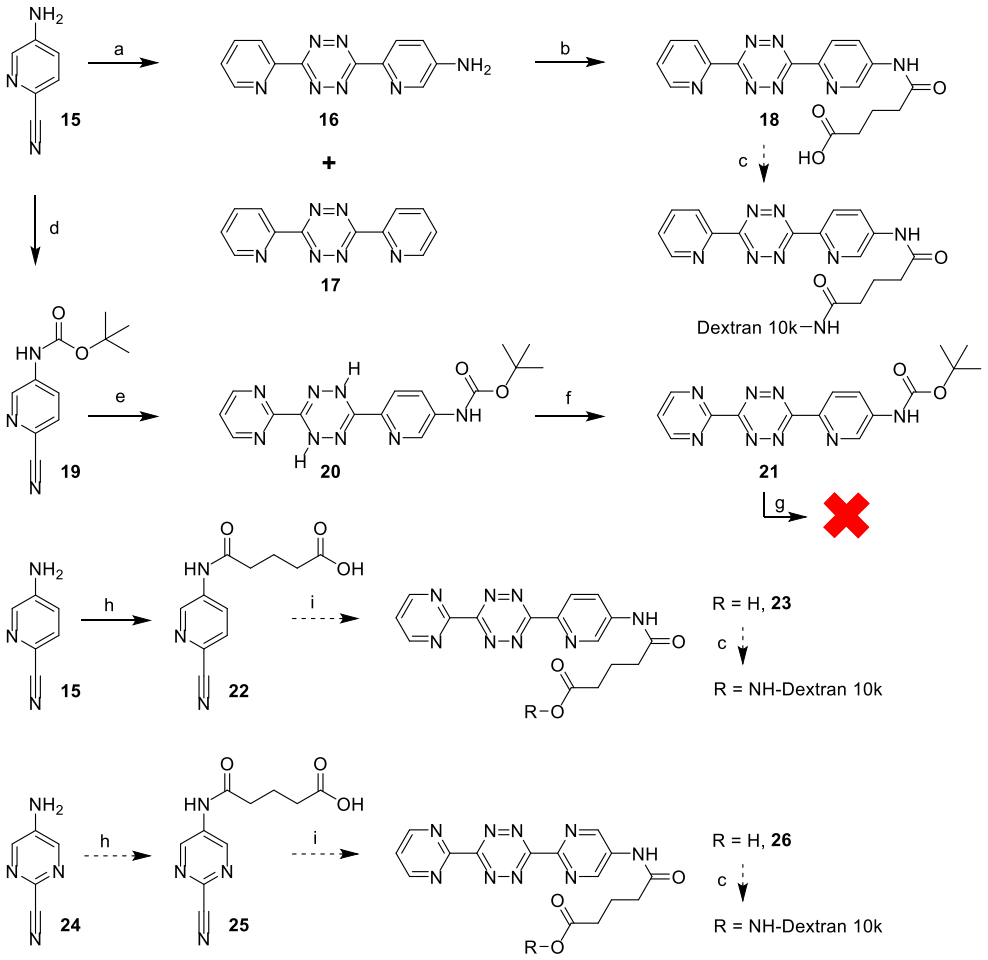

Scheme 2 Attempted and projected syntheses of electron poor tetrazines for polymer conjugation. Reagents/conditions: (a) *i.* 2-pyridine carbonitrile, hydrazine hydrate, 90°C, 59%. *ii.* BAIB, DCM, rt, 10% (**16**); (b) glutaric anhydride, THF, 70°C, 64%; (c) amino dextran 10kDa, N-methyl morpholine, PyBOB, DMSO, rt; (d) Boc_2O, Et_3N, DMAP, THF, 60°C, 46%; (e) pyrimidine-2-carbonitrile, hydrazine hydrate, dioxane, 90°C, 43%; (f) BAIB, DCM, rt, 72%; (g) HCl, dioxane, rt; (h) glutaric anhydride, dioxane, 80°C, 80% (**22**); (i) *i.* pyrimidine-2-carbonitrile, hydrazine hydrate, 90°C. *ii.* BAIB, DCM, rt.

Chapter 5 describes the design and synthesis of TCO caged derivatives of α-galactosylceramide (αGalCer; Scheme 3A, **27**) and α-galactosylphytosphingosine (αGalPhs; Scheme 3A, **28**). The self-adjuvanting strategy by Painter, Hermans and co-workers,[19] where an inactive pro-αGalcer rearranges into αGalcer upon esterase or protease activity, formed the basis for the design of this approach to obtain chemically induced activation of invariant natural killer T-cells (iNKT cells). It was reasoned that the amine functionality of αGalPhs could be protected as a TCO carbamate and that subsequent acylation with hexacosanoic acid would result in a TCO caged pro-αGalcer. Key steps in the synthesis included an α-selective glycosylation under NIS/TMSOTf activation, using a 2,3-TBS-4,6-DTBS protected thiogalactoside donor and a 2-azido-3,4-cyclic carbonate protected phytosphingosine acceptor, followed by hydrogenation, TCO carbamate formation and saponification. Direct desilylation afforded the TCO protected αGalPhs (**28**), whereas esterification and subsequent deprotection gave the TCO protected pro-αGalcer (**27**).

Pending the immunological evaluation of compounds **27** and **28** in presence and absence of a tetrazine activator, it would be of interest to attach an MHC-I peptide antigen onto the caged glycolipid, thereby obtaining a covalent glycolipid-peptide vaccine which can be activated using 'click to release' chemistry. This would be synthetically feasible by combining the established synthetic route of Chapter 5 with the bifunctional TCO presented in Chapter 2 (**1**) and 2-(aminooxy)acetyl-FFRKSIINFEKL[19] to obtain αGalPhs-TCO-FFRKSIINFEKL (Scheme 3B, **29**). Functionalization of α-galactosylated azido phytosphingosine **30** would have to be slightly adjusted towards this synthetic strategy. Saponification of **30** to obtain diol **31** would be followed by Staudinger reduction of the azide to obtain **32**. This would then allow the introduction of the bifunctional TCO moiety to obtain **33** without inducing hydrolysis of the sterically hindered NHS-ester under alkaline conditions. Desilylation may then afford intermediate **34**, which can subsequently undergo selective conjugation of the NHS-ester with the hydroxylamine functionality to obtain **29**. Additionally, it would be of interest to extend this proposed synthetic scheme with the regioselective acylation of **33** in the presence of hexacosonoic acid to obtain **35**. Organoborinate catalysis[20–22] may offer enhanced conversion and regioselectivity for this step without compromising the NHS-ester. Desilylation would then afford **36**, which can undergo selective hydroxylamine conjugation to obtain αGalCer-TCO-FFRKSIINFEKL (**37**).

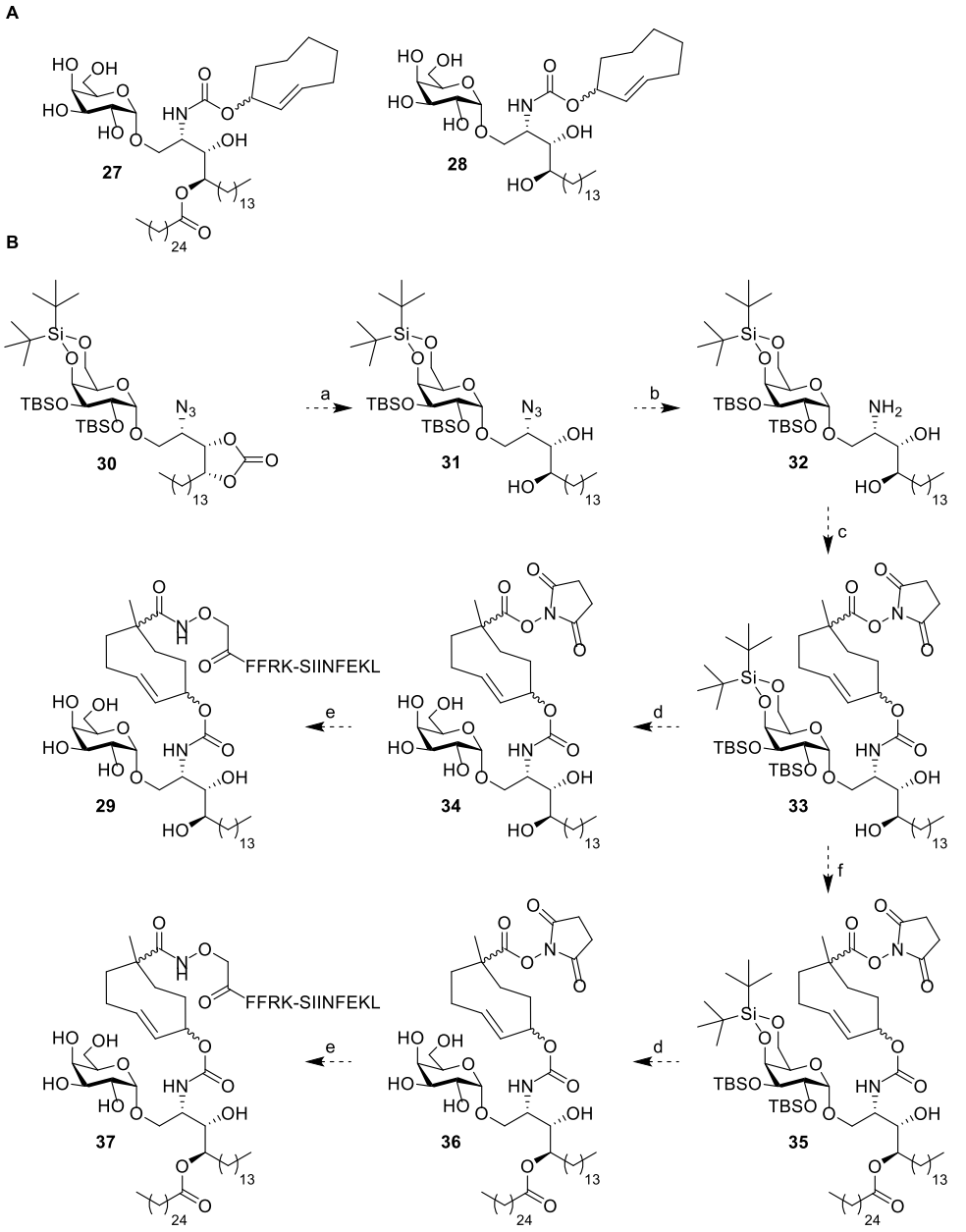

Scheme 3 A) TCO caged αGalcer (**27**) and αGalPhs (**28**) probes described in Chapter 5. B) Proposed synthesis of a TCO caged αGalPhs-MHC-I peptide conjugate (**29**) and αGalCer-MHC-I peptide conjugate (**37**). Reagents/conditions: (a) LiOH, THF, H_2O, 0° to rt; (b) *i.* trimethylphosphine, THF, rt. *ii.* NaOH, H_2O, rt; (c) **1**, DIPEA, DMF, rt; (d) $Et_3N \cdot 3HF$, THF, rt; (e) 2-(aminooxy)acetyl-FFRKSIINFEKL, MeOH, THF, H_2O, rt; (f) *i.* hexacosanoic acid, EDC · HCl, DIPEA, THF. *ii.* **33**, 2-aminoethyl diphenylborinate.

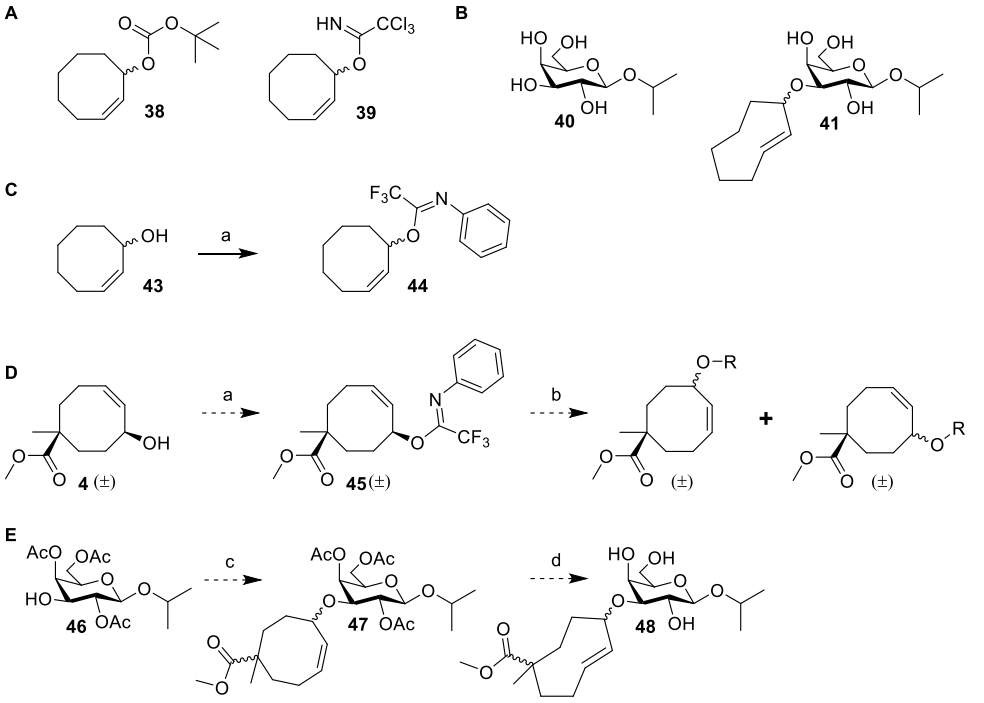

Scheme 4 A) Cyclooctene reagents **38** and **39** employed in Chapter 6 for the synthesis of allylic TCO-ethers. B) *lac* operon inducer **40** and caged *lac* operon inducer **41** described in Chapter 6. C) Synthesis of trifluoroimidate **44** from **43**. D) Proposed synthesis of bifunctional trifluoroimidate **45** from **4** and subsequent investigation of stereo- and regioselectivity upon activation in the presence of a Lewis acid. E) Proposed synthesis of caged *lac* operon inducer **48** from **46**. Reagents/conditions: (a) NaH, (Z)-2,2,2,-trifluoro-*N*-phenylacetimidoyl chloride, THF, 0°C to rt, 83% (**44**); (b) TfOH, R-OH, DCM, -40°C to rt; (c) **45**, TfOH, DCM, -40°C to rt; (d) *i.* methyl benzoate, hν (254 nm), Et_2O/isopropanol, rt. ii. NaOMe, MeOH, rt.

Chapter 6 reports synthetic methodology towards allylic TCO-ethers by employing two novel reagents (Scheme 4A, **38** and **39**). Cyclooctene *tert*-butyl carbonate **38** was designed to afford CCO-ethers upon reaction with phenols under palladium catalysis whereas Lewis acid triggered activation of cyclooctene trichloroimidate **39** afforded CCO-ethers from aliphatic alcohols. Subsequently, photochemical isomerization of the CCO-ether affords the corresponding TCO-ether. The activity of a novel *lac* operon inducer (IPG, Scheme 4B, **40**) was manipulated by attaching a TCO-ether moiety to the 3-OH position, thereby obtaining 3-TCO-IPG (**41**). Recombinant expression experiments in *E. coli* revealed **41** did not affect expression levels in the absence of 3,6-dimethyl-tetrazine (**42**), whereas deprotection of **41** in the presence of **42** was able to switch on recombinant protein expression.

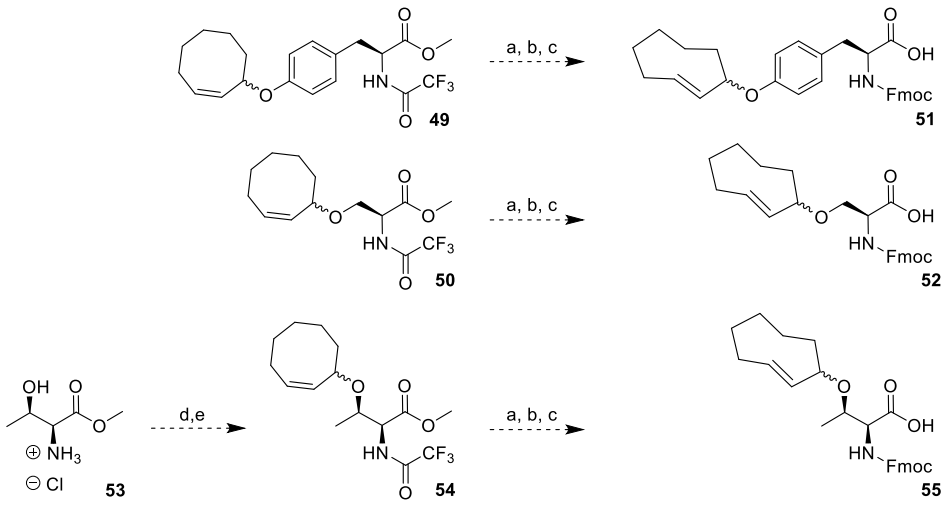

Scheme 5 Proposed synthesis of TCO-ether protected amino acids for Fmoc SPPS. Reagents/conditions: (a) methyl benzoate, hν (254 nm), Et_2O/isopropanol, rt; (b) KOH, MeOH, H_2O, rt; (c) Fmoc-OSu, Na_2CO_3, dioxane, H_2O, rt; (d) ethyl trifluoroacetate, Et_3N, MeOH, 0°C to rt; (e) **39**, TfOH, DCM, -40°C to rt.

It would be of interest to further improve the Lewis acid promoted formation of CCO-ethers from aliphatic alcohols. One way to achieve this is to slow down competing elimination and rearrangement pathways by employing a more stabilized cyclooctene electrophile. To this end, cyclooctenol **43** (Chapter 3 and 6) was reacted with (Z)-2,2,2,-trifluoro-*N*-phenylacetimidoyl chloride in the presence of NaH to obtain cyclooctene trifluoroimidate **44** in 83% yield (Scheme 4C). The conversion of substituted cyclooctenes into CCO ethers would certainly demand a higher efficiency for the corresponding CCO imidates and additionally offers the possibility to examine the stereo- and regioselectivity of these transformations (Scheme 4D). For instance, the conversion of cyclooctene methyl ester **4** into cyclooctene imidate **45** would allow activation with TfOH and a model nucleophile to examine the subsequent stereo- and regiochemical outcomes. Additionally, **45** could be employed to alkylate **46** to obtain **47**, which could be subjected to photochemical isomerization and deacetylation obtain **48** (Scheme 4E). It would be of interest to evaluate whether **48** is able to act as an allosteric *lac* operon antagonist prior to IEDDA pyridazine elimination to form the agonist **40**.

Provided the updated Fmoc SPPS-based strategy for TCO-modified peptide synthesis (Figure 2) works as intented, the CCO-ethers of L-tyrosine and L-serine (Scheme 5, **49** and **50**) described in Chapter 6 could be subjected to photochemical isomerization, alkaline deprotection[23] and Fmoc functionalization to obtain Fmoc-protected TCO-ether amino acids **51** and **52**. It would also be of interest to subject L-threonine methyl

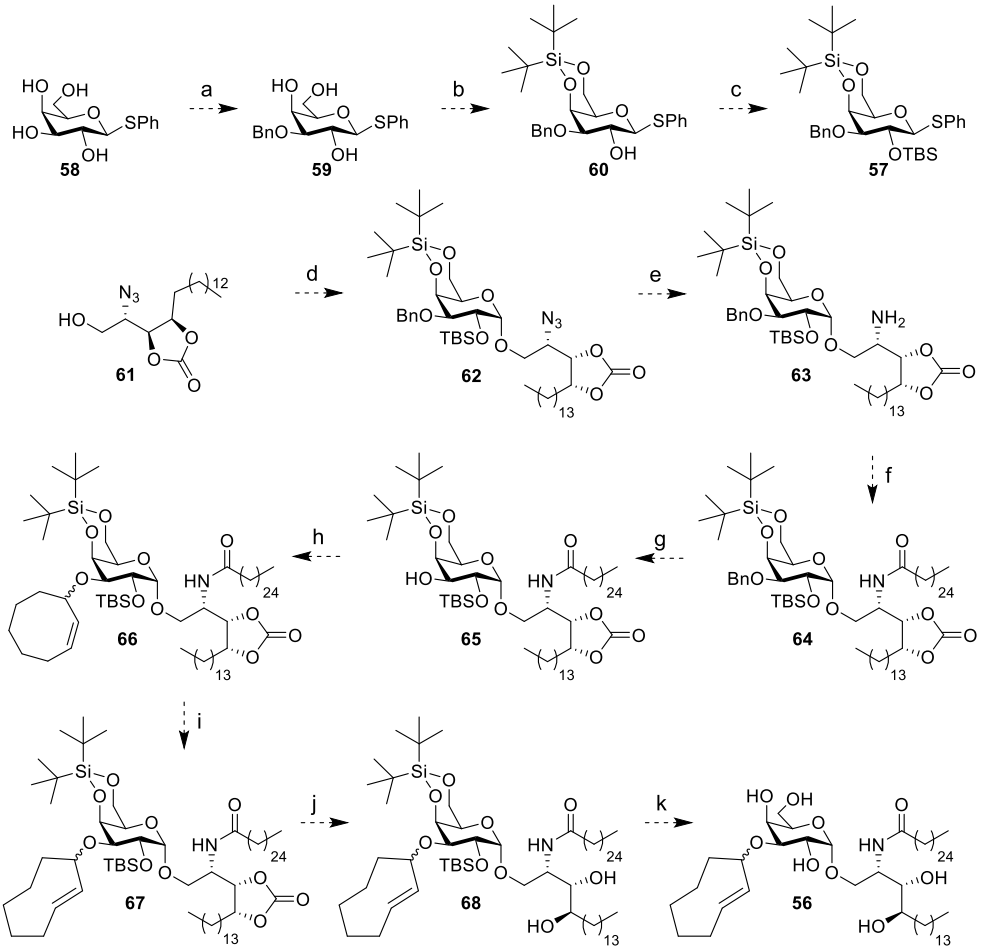

Scheme 6 Proposed synthesis of TCO-ether protected αGalcer (**56**). Reagents/conditions: (a) i. Bu_2SnO, toluene, 105°C; ii. benzyl bromide, TBABr, toluene, 70°C; (b) $DTBS(OTf)_2$, pyridine, DMF, -40°C; (c) TBS-OTf, DMAP, pyridine, 0°C to rt; (d) **57**, NIS, TMS-OTf, DCM, -40°C; (e) PtO_2, H_2 (g), THF, rt; (f) hexacosonoic acid, EDC · HCl, DIPEA, DMAP, DCM; (g) $Pd(OH)_2/C$, H_2 (g), EtOAc, rt; (h) **39** or **44**, TfOH, DCM, -40°C to rt; (i) methyl benzoate, hν (254 nm), Et_2O/isopropanol, rt; (j) LiOH, THF, H_2O, rt; (k) Et_3N · 3HF, THF, rt.

ester **53** to N-trifluoroacetyl protection[24] and subsequent CCO-etherification to obtain **54**, which can also be transformed into the corresponding Fmoc-protected TCO-ether amino acid (**55**). It is conceivable that competing β-elimination necessitates a modified protecting group strategy for compounds **52** and **55**.

The synthesis of a TCO-ether protected αGalcer derivative (**56**) would provide a means to directly interfere with recognition of the exposed galactose moiety in the CD1d-TCR interface (Scheme 6). Orthogonally protected thioglycoside donor (**57**) could be

accessed from thioglycoside **58** by regioselective introduction of a benzyl group using stannylene-acetal chemistry to obtain **59**,[25,26] followed by installation of the 4,6-DTBS protecting group to give **60**. Silylation in the presence of TBSOTf would then provide **57**. NIS/TMSOTf-mediated glycosylation between **57** and **61** (Chapter 5) would afford intermediate **62**, which can be selectively hydrogenated in the presence of PtO_2 to obtain **63**. Installation of the amide bond to obtain **64** would be followed by hydrogenation in the presence of Pearlman's catalyst to obtain **65**. Installation of the CCO-ether moiety in the presence of cyclooctene imidates **39** or **44** and TfOH would give **66**, which is amenable for photoisomerization towards TCO-ether **67**. Saponification of the cyclic carbonate moiety would afford **68** and subsequent desilylation would result in TCO-ether protected αGalcer **56**.

7.2 Experimental procedures

General methods: Commercially available reagents and solvents were used as received. Moisture and oxygen sensitive reactions were performed under N_2 atmosphere (balloon). DCM, toluene, THF, dioxane and Et_2O were stored over (flame-dried) 4 Å molecular sieves (8-12 mesh). Methanol was stored over (flame-dried) 3 Å molecular sieves. DIPEA and Et_3N were stored over KOH pellets. TLC analysis was performed using aluminum sheets, pre-coated with silica gel (Merck, TLC Silica gel 60 F_{254}). Compounds were visualized by UV absorption (λ = 254 nm), by spraying with either a solution of $KMnO_4$ (20 g/L) and K_2CO_3 (10 g/L) in H_2O, a solution of $(NH_4)_6Mo_7O_{24} \cdot 4H_2O$ (25 g/L) and $(NH_4)_4Ce(SO_4)_4 \cdot 2H_2O$ (10 g/L) in 10% H_2SO_4, 20% H_2SO_4 in EtOH, or phosphomolybdic acid in EtOH (150 g/L), where appropriate, followed by charring at ca. 150°C. Column chromatography was performed on Screening Devices b.v. Silica Gel (particle size 40-63 μm, pore diameter 60 Å). Celite Hyflo Supercel (Merck) was used to impregnate the reaction mixture prior to silica gel chromatography when indicated. ^1H, ^{13}C APT, ^1H COSY, HSQC and HMBC spectra were recorded with a Bruker AV-400 (400/100 MHz) spectrometer. Chemical shifts are reported as δ values (ppm) and were referenced to tetramethylsilane (δ = 0.00 ppm) or the residual solvent peak as internal standard. *J* couplings are reported in Hz.

LC-MS analysis was performed on a Finnigan Surveyor HPLC system (detection at 200-600 nm) with an analytical C_{18} column (Gemini, 50 x 4.6 mm, 3 μm particle size, Phenomenex) coupled to a Finnigan LCQ Advantage MAX ion-trap mass spectrometer (ESI^+). The applied buffers were H_2O, MeCN and 1.0% TFA in H_2O (0.1% TFA end concentration). HPLC purification was performed on a Gilson HPLC system (detection at 214 nm) coupled to a semi-preparative C_{18} column (Gemini, 250 x 10 mm, 5 μm particle size, Phenomenex). The applied buffers were H_2O, MeCN and 100 mM NH_4OAc in H_2O (10 mM NH_4OAc end concentration). High resolution mass spectra were recorded by direct injection (2 μL of a 1 μM solution in H_2O/MeCN 1:1 and 0.1% formic acid) on a mass spectrometer (Q Exactive HF Hybrid Quadrupole-Orbitrap) equipped with an electrospray ion source in positive mode (source voltage 3.5 kV, sheath gas flow 10, capillary temperature 275°C) with resolution R = 240,000 at m/z 400 (mass range m/z = 160-2,000) and an external lock mass. The high resolution mass spectrometer was calibrated prior to measurements with a calibration mixture (Thermo Finnigan).

Preparation of neutralized silica gel: Unmodified silica gel (500 gram) was slowly dispersed into a 3 L round-bottom flask containing a stirring volume of H_2O (1.7 L). NH_4OH (28% w/w, 100 mL) was added and the alkaline suspension was stirred for 30 min. The suspension was filtered, washed with H_2O and the silica gel was dried on aluminium foil overnight at rt. The silica was transferred into a glass container and remaining traces of H_2O were removed by drying in an oven at 150°C overnight.

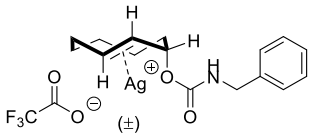

Silver trifluoroacetate complex of axial TCO carbamate 12 (69): An NMR tube was charged with silver trifluoroacetate (19.9 mg, 90 µmol, 1.5 equiv). Axial TCO-carbamate **12** (Chapter 3; 15.5 mg, 60 µmol, 1.0 equiv) was dissolved in $CDCl_3$ (600 µL) and the solution was added to the NMR tube. After vortexing, a diastereomeric mixture of axial TCO carbamate-Ag complexes **69** (**69$_A$** : **69$_B$**, 0.55 : 0.40) was observed: ^{1}H NMR (400 MHz, $CDCl_3$) δ 7.43 (t, *J* = 5.6 Hz, 1NH, **69$_A$**), 7.37 – 7.21 (m, 5H, **69$_A$** + **69$_B$**), 6.17 – 5.99 (m, 1H, **69$_B$**), 5.81 (d, *J* = 15.9 Hz, 1H, **69$_B$**), 5.70 (d, *J* = 15.8 Hz, 1H, **69$_A$**), 5.53 (t, *J* = 5.8 Hz, 1NH, **69$_B$**), 5.40 (s, 1H, **69$_B$**), 5.21 (s, 1H, **69$_A$**), 5.12 – 4.93 (m, 1H, **69$_A$**), 4.42 – 4.12 (m, 2H, **69$_A$** + **69$_B$**), 2.66 (d, *J* = 8.6 Hz, 1H, **69$_B$**), 2.40 (d, *J* = 11.6 Hz, 1H, **69$_A$**), 2.19 – 1.50 (m, 6H, **69$_A$** + **X$_B$**; 1H, **69$_B$**), 1.32 – 1.16 (m, 1H, **69$_A$**), 1.12 – 0.98 (m, 1H, **69$_B$**), 0.92 – 0.61 (m, 1H, **69$_A$** + **69$_B$**; 1H, **69$_A$**); ^{13}C NMR (101 MHz, $CDCl_3$) δ 162.5 (q, *J* = 35.2 Hz; TFA), 157.7, 156.1, 139.2, 138.1, 128.8 (x4), 127.7, 127.6, 127.5, 127.1 (x3), 121.4, 120.3, 119.1, 118.3, 117.4 (q, *J* = 290.8 Hz; TFA), 75.2, 74.2, 45.6, 45.2, 40.7, 40.3, 36.4, 36.1, 36.1, 35.7, 28.2, 28.1, 23.3 (x2).

**Note: After 72 h the diastereomeric mixture of axial TCO carbamate-Ag complexes was analyzed once again with NMR to obtain identical ^{1}H and ^{13}C spectra.*

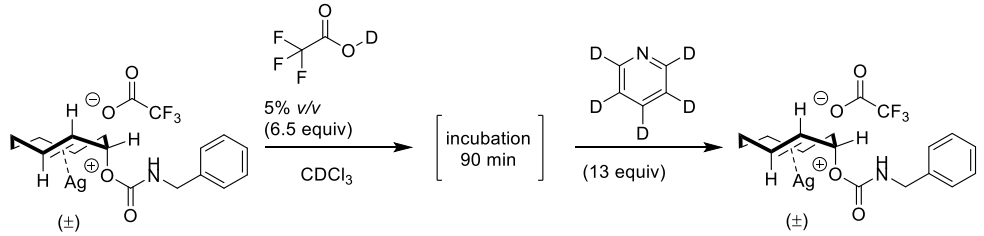

Stability NMR experiment with silver trifluoroacetate complex of axial TCO carbamate 12 (69) - 5% *v/v* TFA-D in DCM - incubation 90 min - quenching with pyridine D_5: Axial TCO-carbamate **12** (Chapter 3; 15.5 mg, 60 µmol, 1.0 equiv) was dissolved in $CDCl_3$ (570 µL) in an NMR tube. After measuring a reference spectrum (^{1}H NMR), silver trifluoroacetate (19.9 mg, 90 µmol, 1.5 equiv) was added. After vortexing for 1 min and measuring a reference spectrum (^{1}H NMR), additional silver trifluoroacetate (19.88 mg, 90 µmol, 1.5 equiv) was added. After vortexing for 1 min and measuring a reference spectrum (^{1}H NMR), TFA-D (30 µL, 0.39 mmol, 6.5 equiv) was added to obtain a 0.1 M solution of **69** in 5% TFA-D (*v/v* in $CDCl_3$). The mixture was vortexed for 1 min, and subsequently characterized with NMR (^{1}H, ^{13}C, COSY, HSQC). After 90 min, the mixture was neutralized by adding pyridine-D_5 (63 µL, 0.78 mmol, 13 equiv), vortexed for 1 min and characterized with NMR (^{1}H, ^{13}C, COSY, HSQC).

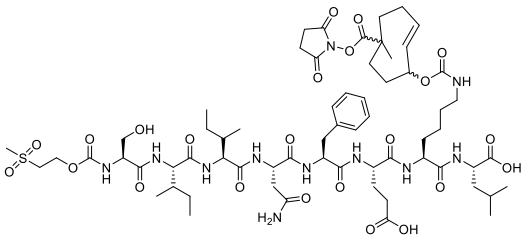

MSc-SIINFEK(NHS-bTCO)L (14): MSc-SIINFEKL (Chapter 4; **13**, 116.8 mg, 105 µmol, 1.0 equiv) and NHS-bTCO (**1**, 52.9 mg, 125 µmol, 1.2 equiv) were combined in a 50 mL tube and dissolved in anhydrous DMF (10 mL) under N_2. Anhydrous DIPEA (73 µL, 418 µmol, 4.0 equiv) was added and

the reaction mixture was shaken for 19 h at room temperature. The tube was shielded with aluminum foil during the reaction. The crude reaction mixture was purified by HPLC (MeCN in H_2O with 10 mM NH_4OAc) to obtain **14** (17.59 mg, 12.0 µmol, 12%) as a solid after lyophilization: LC-MS (linear gradient 10 → 90% MeCN, 0.1% TFA, 12.5 min): R_t (min): 6.39 (ESI-MS (m/z): 1420.27 ($M+H^+$)); HRMS: calculated for $C_{64}H_{99}N_{11}O_{23}S$ 710.83125 $[M+2H]^{2+}$; found 710.83120.

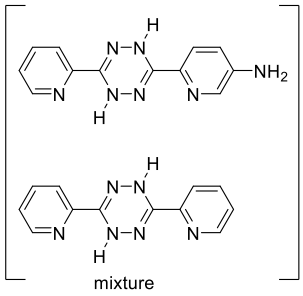

Dihydrotetrazines 70 and 71: Synthesis was performed according to a modified procedure.[16] 2-Pyridine carbonitrile (2.78 mL, 28.8 mmol, 1.0 equiv), 5-amino-2-pyridine carbonitrile (**15**, 3.43 g, 28.8 mmol, 1.0 equiv) and hydrazine monohydrate (5.59 mL, 115 mmol, 4.0 equiv) were combined in a microwave tube. The tube was briefly purged with N_2 before capping the tube and stirring the reaction mixture at 90°C (oil bath) for 16 h. Subsequently, the reaction mixture was cooled to 0°C (ice bath). A precipitate formed, which was collected by filtration and rinsed with cold H_2O. The filtrate was cooled to 0°C (ice bath) and additional precipitate was collected by filtration. The residue was co-evaporated with toluene (3x) to obtain the crude mixture of dihydrotetrazines **70** and **71** (4.31 g, ≥ 17.02 mmol, 59%) as an orange solid which was used for the next step without further purification.

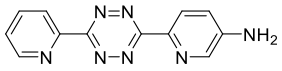

Tetrazine 16: Synthesis was performed according to a modified procedure.[16] The crude mixture of dihydrotetrazines **70** and **71** described in the previous step (1.00 g, 3.95 mmol, 1.0 equiv) was suspended in anhydrous DCM (50 mL) before adding (Diacetoxyiodo)benzene (BAIB, 2.60 g, 8.07 mmol, 2.0 equiv). The reaction mixture was stirred for 3 h at room temperature. The crude reaction mixture was applied directly onto a silica gel column (neutralized silica gel) and purified using column chromatography (DCM → 1% MeOH in DCM → 1.5 % MeOH in DCM) to obtain **16** (104 mg, 0.41 mmol, 10%) as a red solid: R_f = 0.2 (5% MeOH in DCM); ^{1}H NMR (400 MHz, DMSO) δ 8.90 (ddd, *J* = 4.7, 1.7, 0.9 Hz, 1H), 8.53 (dt, *J* = 7.9, 1.0 Hz, 1H), 8.36 (d, *J* = 8.6 Hz, 1H), 8.23 (d, *J* = 2.7 Hz, 1H), 8.12 (td, *J* = 7.8, 1.8 Hz, 1H), 7.69 (ddd, *J* = 7.6, 4.7, 1.1 Hz, 1H), 7.13 (dd, *J* = 8.7, 2.8 Hz, 1H), 6.39 (s, 2NH); ^{13}C NMR (101 MHz, DMSO) δ 162.9, 162.6, 150.5, 148.0, 137.7, 137.2, 136.0, 126.2, 125.7, 123.7, 119.0. Spectroscopic data was in agreement with literature.[17,27,28]

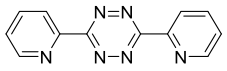

Tetrazine 17: This compound was encountered as a crude byproduct during column chromatography purifications of compound **16**. Purification using silica gel chromatography (DCM → 1% MeOH in DCM) afforded **17** as a pink solid: R_f = 0.3 (5% MeOH in DCM); ^{1}H NMR (400 MHz, DMSO) δ 8.99 – 8.91 (m, 2H), 8.62 (d, *J* = 7.9 Hz, 2H), 8.17 (td, *J* = 7.8, 1.7 Hz, 2H), 7.74 (ddd, *J* = 7.6, 4.7, 1.0 Hz, 2H); ^{13}C NMR (101 MHz, DMSO) δ 163.3 (x2), 150.7 (x2), 150.1 (x2), 137.9 (x2), 126.7 (x2), 124.4 (x2); ^{1}H NMR (400 MHz, $CDCl_3$) δ 9.05 – 8.96 (m, 2H), 8.81 – 8.73 (m, 2H), 8.03 (td, *J* = 7.8, 1.7 Hz, 2H), 7.60 (ddd, *J* = 7.6, 4.8, 1.0 Hz, 2H); ^{13}C NMR (101 MHz, $CDCl_3$) δ 164.0 (x2), 151.2 (x2), 150.2 (x2), 137.7 (x2), 126.8 (x2), 124.7 (x2). Spectroscopic data was in agreement with literature.[1]

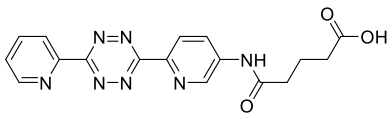

Tetrazine 18: Synthesis was performed according to a modified procedure.[27] Tetrazine **16** (30 mg, 0.119 mmol, 1.0 equiv) and glutaric anhydride (68 mg, 0.597 mmol, 5.0 equiv) were combined in a 25 mL round-bottom flask and suspended in anhydrous dioxane (7 mL) under N_2. The flask was sealed and the reaction mixture was stirred for 48 h at 60°C (oil bath). Additional glutaric anhydride (68 mg, 0.60 mmol, 5.0 equiv) was added and the reaction mixture was stirred for 48 h at 70°C (oil bath). The crude reaction mixture was concentrated *in vacuo* and purified by successive sonication, centrifugation and decanting steps in anhydrous DCM (3 x 14 mL) and distilled EtOAc (14 mL), respectively, to obtain **18** (28 mg, 77 µmol, 64%) as a pink solid: LC-MS (linear gradient 0 → 50% MeCN, 0.1% TFA, 12.5 min): R_t (min): 6.67 (ESI-MS (m/z): 366.07 ($M+H^+$)); ^{1}H NMR (400 MHz, DMSO) δ 12.14 (br s, 1OH), 10.58 (s, 1NH), 9.04 (d, *J* = 2.2 Hz, 1H), 8.93 (d, *J* = 4.3 Hz, 1H), 8.60 (dd, *J* = 11.5, 8.3 Hz, 2H), 8.43 (dd, *J* = 8.7, 2.4 Hz, 1H), 8.15 (td, *J* = 7.8, 1.5 Hz, 1H), 7.72 (dd, *J* = 7.8, 4.7 Hz, 1H), 2.47 (t, *J* = 7.3 Hz, 2H), 2.32 (t, *J* = 7.3 Hz, 2H), 1.86 (p, *J* = 7.3 Hz, 2H); ^{13}C NMR (101 MHz, DMSO) δ 172.0, 163.1, 162.8, 150.6, 150.2, 143.8, 141.3, 138.5, 137.8, 126.6, 126.2, 124.9, 124.2, 35.4, 32.9, 20.2. Spectroscopic data was in agreement with literature.[27]

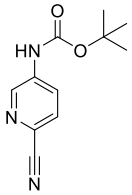

Carbonitrile 19: 5-Amino-2-pyridine carbonitrile (**15**, 1.19 g, 10.0 mmol, 1.0 equiv) was dissolved in anhydrous THF (12 mL) under N_2. The solution was cooled to 0°C (ice bath) before adding Et_3N (6.97 mL, 50.0 mmol, 5.0 equiv), DMAP (61 mg, 0.5 mmol, 5 mol%) and Boc_2O (2.32 mL, 10.0 mmol, 1.0 equiv). The reaction mixture was gradually heated to 60°C (oil bath) and stirred for 20 h. The reaction mixture was diluted with H_2O (10 mL) and extracted with EtOAc (10 mL). The organic layer was dried over $MgSO_4$, filtered and concentrated *in vacuo*. The crude product was purified by silica gel chromatography (5% EtOAc in pentane → 20% EtOAc in pentane) to obtain **19** (1.00 g, 4.56 mmol, 46%) as a white solid: R_f = 0.5 (10% EtOAc in pentane); ^{1}H NMR (400 MHz, DMSO) δ 10.15 (s, 1NH), 8.73 (d, *J* = 2.4 Hz, 1H), 8.11 – 8.02 (m, 1H), 7.92 (dd, *J* = 8.6, 3.0 Hz, 1H), 1.49 (s, 9H); ^{13}C NMR (101 MHz, DMSO) δ 152.4, 141.0, 139.7, 129.6, 124.8, 124.3, 117.8, 80.7, 27.9 (x3).

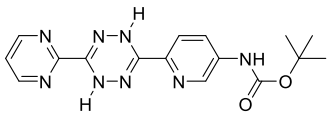

Dihydrotetrazine 20: Carbonitrile **19** (110 mg, 0.5 mmol, 1.0 equiv), pyrimidine-2-carbonitrile (53 mg, 0.5 mmol, 1.0 equiv), dioxane (98 µL) and hydrazine monohydrate (98 µL, 2.0 mmol, 4.0 equiv) were combined in a microwave tube. The tube was briefly purged with N_2 before capping the tube and stirring the reaction mixture at 90°C (oil bath) for 19 h. An orange precipitate had formed, which was suspended in cold H_2O, filtered, washed with cold H_2O and dried *in vacuo*. The crude product was dissolved in THF, impregnated with Celite and concentrated *in vacuo*. The impregnated crude product was purified by silica gel chromatography (DCM → 3% MeOH in DCM) to obtain **20** (76 mg, 0.21 mmol, 43%) as an orange solid: R_f = 0.5 (3% MeOH in DCM); ^{1}H NMR (400 MHz, DMSO) δ 9.89 (s, 1NH), 9.03 (s, 1H), 8.92 (d, *J* = 4.9 Hz, 2H), 8.87 (s, 1H), 8.67 (d, *J* = 1.9 Hz, 1H), 8.03 (dd, *J* = 8.8, 2.5 Hz, 1H), 7.89 (d, *J* = 8.6 Hz, 1H), 7.61 (t, *J* = 4.9 Hz, 1H), 1.49 (s, 9H).

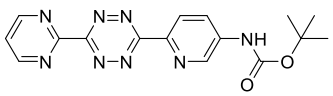

Tetrazine 21: Dihydrotetrazine **20** (76 mg, 0.21 mmol, 1.0 equiv) was suspended in anhydrous DCM (1.0 mL) before adding (Diacetoxyiodo)benzene (BAIB, 104 mg, 0.32 mmol, 1.5 equiv). The reaction mixture was stirred for 2 h at room temperature and was subsequently concentrated *in vacuo.* The crude product was purified by silica gel chromatography (DCM → 3% MeOH in DCM) to obtain **21** (54 mg, 0.153 mmol, 72%) as a red solid: R_f = 0.3 (2% MeOH in DCM); ^{1}H NMR (400 MHz, DMSO) δ 10.14 (s, 1NH), 9.20 (d, *J* = 4.8 Hz, 2H), 8.99 – 8.89 (m, 1H), 8.62 (d, *J* = 8.7 Hz, 1H), 8.26 (d, *J* = 8.5 Hz, 1H), 7.83 (t, *J* = 4.7 Hz, 1H), 1.53 (s, 9H); ^{13}C NMR (101 MHz, DMSO) δ 162.9, 162.8, 159.2, 158.6 (x2), 152.7, 142.8, 140.7, 139.3, 125.4, 125.0, 123.1, 80.6, 28.1 (x3).

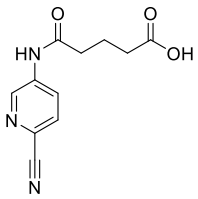

Carbonitrile 22: Synthesis was performed according to a modified procedure.[18] 5-Amino-2-pyridine carbonitrile (**15**, 596 mg, 5.00 mmol, 1.0 equiv) and glutaric anhydride (2.85 g, 25.0 mmol, 5.0 equiv) were combined in a 100 mL round-bottom flask and suspended in anhydrous dioxane (20 mL) under N_2. The flask was sealed and the reaction mixture was stirred for 72 h at 80°C (oil bath). The reaction mixture was allowed to cool down to room temperature and was subsequently concentrated *in vacuo*. The crude product was refluxed in anhydrous MeOH to precipitate the product, followed by filtration. The residue was collected and the filtrate was allowed to crystallize overnight to collect additional residue. Carbonitrile **22** (937 mg, 4.02 mmol, 80%) was obtained as a solid: ^{1}H NMR (400 MHz, DMSO) δ 10.67 (s, 1NH), 8.84 (d, *J* = 2.6 Hz, 1H), 8.26 (dd, *J* = 8.6, 2.6 Hz, 1H), 7.96 (d, *J* = 8.6 Hz, 1H), 2.44 (t, *J* = 7.4 Hz, 2H), 2.26 (t, *J* = 7.3 Hz, 2H), 1.80 (p, *J* = 7.3 Hz, 2H); ^{13}C NMR (101 MHz, DMSO) δ 174.3, 172.3, 141.8, 139.1, 129.7, 125.7, 125.6, 117.8, 35.5, 33.1, 20.2. Spectroscopic data was in agreement with literature.[18]

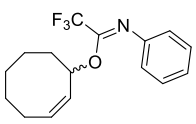

Cyclooctene reagent 44: Cyclooctenol **43** (Chapter 3 and 6; 138 mg, 1.09 mmol, 1.0 equiv) was dissolved in anhydrous THF (1.0 mL) under N_2. The solution was cooled to 0°C (ice bath) before adding sodium hydride (70 mg, 1.75 mmol, 1.6 equiv). After 15 min, (Z)-2,2,2,-trifluoro-N-phenylacetimidoyl chloride (309 mg, 1.49 mmol, 1.4 equiv) was dissolved in anhydrous THF (2.0 mL) under N_2 and was slowly added to the reaction mixture. The reaction mixture was stirred for 16 h and allowed to warm to room temperature. The reaction mixture was concentrated *in vacuo* and the crude product was purified by silica gel chromatography (pentane → 2% Et_2O in pentane) to obtain **44** (269 mg, 0.91 mmol, 83%) as a yellow oil: R_f = 0.8 (2% Et_2O in pentane); ^{1}H NMR (400 MHz, $CDCl_3$) δ 7.33 – 7.19 (m, 2H), 7.10 – 6.98 (m, 1H), 6.80 (d, *J* = 7.8 Hz, 2H), 5.78 (br s, 1H), 5.68 (q, *J* = 9.1, 8.4 Hz, 1H), 5.62 – 5.47 (m, 1H), 2.38 – 1.85 (m, 3H), 1.76 – 1.22 (m, 7H); ^{13}C NMR (101 MHz, $CDCl_3$) δ 144.8, 130.4, 130.1, 128.8 (x2), 123.8, 119.7 (x2), 116.5 (q, *J* = 285.2 Hz), 76.2, 34.5, 28.8, 26.5, 25.9, 23.3.

*Note: the ^{13}C signal associated with the imidate moeity (C=O) was not reported due to a lack of resolution in the spectrum of **44**.*

7.3 References

[1] R. M. Versteegen, R. Rossin, W. ten Hoeve, H. M. Janssen, M. S. Robillard, *Angew. Chem. Int. Ed.* **2013**, *52*, 14112–14116.

[2] J. Li, P. R. Chen, *Nat. Chem. Biol.* **2016**, *12*, 129–137.

[3] K. Neumann, A. Gambardella, M. Bradley, *ChemBioChem* **2019**, *20*, 872–876.

[4] J. Tu, M. Xu, R. M. Franzini, *ChemBioChem* **2019**, *20*, 1615–1627.

[5] R. Rossin, S. M. J. van Duijnhoven, W. ten Hoeve, H. M. Janssen, F. J. M. Hoeben, R. M. Versteegen, M. S. Robillard, *Bioconjug. Chem.* **2016**, *27*, 1697–1706.

[6] M. A. R. Geus, E. Maurits, A. J. C. Sarris, T. Hansen, M. S. Kloet, K. Kamphorst, W. Hoeve, M. S. Robillard, A. Pannwitz, S. A. Bonnet, J. D. C. Codée, D. V. Filippov, H. S. Overkleeft, S. I. Kasteren, *Chem. Eur. J.* **2020**, *26*, 9900–9904.

[7] G. R. Ediriweera, J. D. Simpson, A. V Fuchs, T. K. Venkatachalam, M. Van De Walle, C. B. Howard, S. M. Mahler, J. P. Blinco, N. L. Fletcher, Z. H. Houston, C. A. Bell, K. J. Thurecht, *Chem. Sci.* **2020**, *11*, 3268–3280.

[8] M. A. Muhs, F. T. Weiss, *J. Am. Chem. Soc.* **1962**, *84*, 4697–4705.

[9] D. L. Cedeño, R. Sniatynsky, *Organometallics* **2005**, *24*, 3882–3890.

[10] A. C. Cope, R. D. Bach, *Org. Synth.* **1969**, *49*, 39.

[11] M. Royzen, G. P. A. Yap, J. M. Fox, *J. Am. Chem. Soc.* **2008**, *130*, 3760–3761.

[12] H. E. Murrey, J. C. Judkins, C. W. Am Ende, T. E. Ballard, Y. Fang, K. Riccardi, L. Di, E. R. Guilmette, J. W. Schwartz, J. M. Fox, D. S. Johnson, *J. Am. Chem. Soc.* **2015**, *137*, 11461–11475.

[13] Y. Fang, J. C. Judkins, S. J. Boyd, C. W. am Ende, K. Rohlfing, Z. Huang, Y. Xie, D. S. Johnson, J. M. Fox, *Tetrahedron* **2019**, *75*, 4307–4317.

[14] S. Du, D. Wang, J.-S. Lee, B. Peng, J. Ge, S. Q. Yao, *Chem. Commun.* **2017**, *53*, 8443–8446.

[15] N. K. Devaraj, G. M. Thurber, E. J. Keliher, B. Marinelli, R. Weissleder, *Proc. Natl. Acad. Sci.* **2012**, *109*, 4762–4767.

[16] R. Selvaraj, J. M. Fox, *Tetrahedron Lett.* **2014**, *55*, 4795–4797.

[17] M. L. Blackman, M. Royzen, J. M. Fox, *J. Am. Chem. Soc.* **2008**, *130*, 13518–13519.

[18] A. Maggi, E. Ruivo, J. Fissers, C. Vangestel, S. Chatterjee, J. Joossens, F. Sobott, S. Staelens, S. Stroobants, P. Van Der Veken, L. Wyffels, K. Augustyns, *Org. Biomol. Chem.* **2016**, *14*, 7544–7551.

[19] R. J. Anderson, C. Tang, N. J. Daniels, B. J. Compton, C. M. Hayman, K. a Johnston, D. a Knight, O. Gasser, H. C. Poyntz, P. M. Ferguson, D. S. Larsen, F. Ronchese, G. F. Painter, I. F. Hermans, *Nat. Chem. Biol.* **2014**, *10*, 943–949.

[20] D. Lee, M. S. Taylor, *J. Am. Chem. Soc.* **2011**, *133*, 3724–3727.

[21] D. Lee, C. L. Williamson, L. Chan, M. S. Taylor, *J. Am. Chem. Soc.* **2012**, *134*, 8260–8267.

[22] M. S. Taylor, *Acc. Chem. Res.* **2015**, *48*, 295–305.

[23] R. M. Versteegen, W. ten Hoeve, R. Rossin, M. A. R. de Geus, H. M. Janssen, M. S. Robillard, *Angew. Chem. Int. Ed.* **2018**, *57*, 10494–10499.

[24] K. Murayama, H. Asanuma, *ChemBioChem* **2017**, *18*, 142–149.

[25] J. G. Taylor, X. Li, M. Oberthür, W. Zhu, D. E. Kahne, *J. Am. Chem. Soc.* **2006**, *128*, 15084–15085.

[26] H. Xu, Y. Lu, Y. Zhou, B. Ren, Y. Pei, H. Dong, Z. Pei, *Adv. Synth. Catal.* **2014**, *356*, 1735–1740.

[27] C. F. Hansell, P. Espeel, M. M. Stamenović, I. A. Barker, A. P. Dove, F. E. Du Prez, R. K. O'Reilly, *J. Am. Chem. Soc.* **2011**, *133*, 13828–13831.

[28] B. L. Oliveira, Z. Guo, O. Boutureira, A. Guerreiro, G. Jiménez-Osés, G. J. L. Bernardes, *Angew. Chem. Int. Ed.* **2016**, *55*, 14683–14687.